

# The structure of $^{70}\text{Fe}$ : Single-particle and collective degrees of freedom

A. Gade,<sup>1,2</sup> R. V. F. Janssens,<sup>3</sup> J. A. Tostevin,<sup>4</sup> D. Bazin,<sup>1,2</sup> J. Belarge,<sup>1,\*</sup> P. C. Bender,<sup>1,†</sup> S. Bottoni,<sup>5,‡</sup> M. P. Carpenter,<sup>5</sup> B. Elman,<sup>1,2</sup> S. J. Freeman,<sup>6</sup> T. Lauritsen,<sup>5</sup> S. M. Lenzi,<sup>7</sup> B. Longfellow,<sup>1,2</sup> E. Lunderberg,<sup>1,2</sup> A. Poves,<sup>8</sup> L. A. Riley,<sup>9</sup> D. K. Sharp,<sup>6</sup> D. Weisshaar,<sup>1</sup> and S. Zhu<sup>5</sup>

<sup>1</sup>*National Superconducting Cyclotron Laboratory, Michigan State University, East Lansing, Michigan 48824, USA*

<sup>2</sup>*Department of Physics and Astronomy, Michigan State University, East Lansing, Michigan 48824, USA*

<sup>3</sup>*Department of Physics and Astronomy, University of North Carolina at Chapel Hill, Chapel Hill, North Carolina 27599, USA and Triangle Universities Nuclear Laboratory, Duke University, Durham, North Carolina 27708, USA*

<sup>4</sup>*Department of Physics, University of Surrey, Guildford, Surrey GU2 7XH, United Kingdom*

<sup>5</sup>*Physics Division, Argonne National Laboratory, Argonne, Illinois 60439, USA*

<sup>6</sup>*School of Physics and Astronomy, University of Manchester, Manchester M13 9PL, United Kingdom*

<sup>7</sup>*Dipartimento di Fisica e Astronomia dell'Università and INFN, Sezione di Padova, I-35131 Padova, Italy*

<sup>8</sup>*Departamento de Física Teórica e IFT-UAM/CSIC,*

*Universidad Autónoma de Madrid, E-28049 Madrid, Spain*

<sup>9</sup>*Department of Physics and Astronomy, Ursinus College, Collegeville, Pennsylvania 19426, USA*

(Dated: December 31, 2018)

Excited states in the neutron-rich  $^{70}\text{Fe}$  nucleus were populated in a one-proton removal reaction from  $^{71}\text{Co}$  projectiles at 87 MeV/nucleon. A new transition was observed with the  $\gamma$ -ray tracking array GRETINA and shown to feed the previously assigned  $4_1^+$  state. In comparison to reaction theory calculations with shell-model spectroscopic factors, it is argued that the new  $\gamma$  ray possibly originates from the  $6_1^+$  state. It is further shown that the Doppler-reconstructed  $\gamma$ -ray spectra are sensitive to the very different lifetimes of the  $2^+$  and  $4^+$  states, enabling their approximate measurement. The emerging structure of  $^{70}\text{Fe}$  is discussed in comparison to LNPS-new large-scale shell-model calculations.

A goal of nuclear science is to achieve an understanding of nuclei and their properties rooted in the fundamental nucleon-nucleon interactions, while demonstrating predictive power for the shortest-lived species located at the fringes of the nuclear chart. In the quest to extrapolate knowledge to the most neutron-rich systems, including those that may remain beyond experimental reach, much can be learned from nuclei with large neutron excess that clearly display the effects of structural evolution away from the valley of stability. Observables measured for such nuclei provide important extrapolation points toward unknown regions and their successful modeling offers critical benchmarks for theory. Specifically, the complex interplay between single-particle and collective degrees of freedom in the nuclear many-body system provides unique and interesting experimental and theoretical challenges.

Neutron-rich  $^{70}\text{Fe}$  is such a nucleus where single-particle structure is impacted by shell evolution, driven by the spin-isospin parts of the nucleon-nucleon force, and where significant quadrupole collectivity develops. In fact,  $^{70}\text{Fe}$  is said to be part of the  $N = 40$  island of inversion [1, 2] where the neutron-rich Fe and Cr nuclei around  $N = 40$  become the most deformed in the region. This is thought to be caused by the strong quadrupole-quadrupole interaction producing a shape transition in which highly correlated, many-particle-many-hole configurations become more bound than the normal-order (spherical) ones [1]. Such islands of inversion are characterized by rapid structural changes and shape coexistence

[2, 3], providing insight into nuclear structure physics far from stability [4].  $^{70}\text{Fe}$  has 12 neutrons more than the heaviest stable iron isotope, while the heaviest one discovered to date is  $^{76}\text{Fe}$  [5], a nucleus predicted to display collectivity and shape coexistence [2] just two protons below  $^{78}\text{Ni}$ . Indeed, within the iron isotopic chain,  $^{70}\text{Fe}$  is located on the path between the  $N = 40$  and  $N = 50$  islands of inversion [2], with the latter remaining a challenge for next-generation rare-isotope facilities presently under construction.  $^{70}\text{Fe}$  has also been used as a seed nucleus in r-process calculations and associated sensitivity studies [6, 7]. Spectroscopic information on  $^{70}\text{Fe}$ , limited to the identification of two states, the first  $2^+$  level and another with a tentative  $4^+$  assignment, comes thus far from the population of excited states in  $\beta$  decay [8] and a  $(p, 2p)$  reaction study [9].

Here, we present the high-resolution spectroscopy of  $^{70}\text{Fe}$  in the direct one-proton removal reaction  $^9\text{Be}(^{71}\text{Co}, ^{70}\text{Fe}+\gamma)\text{X}$  at 87 MeV/u, leading to a newly observed  $\gamma$ -ray transition and the determination of partial cross sections. The latter are discussed quantitatively in comparison to eikonal reaction theory [10] with LNPS-new shell-model spectroscopic factors [1, 11]. The rather simple  $^{70}\text{Fe}$   $\gamma$ -ray spectrum observed, with only three peaks, is at odds with the predicted strong population of highly-excited states. On the experimental side, we propose, as a solution to this puzzle, the so-called pandemonium effect [12] arising from a sizable fragmentation of the proton spectroscopic strength in  $^{70}\text{Fe}$ . This fragmentation is larger than predicted within the lim-

ited configuration spaces of shell-model calculations, on the theoretical side. While such challenges may actually be rather universal for  $\gamma$ -ray tagged direct reactions leading to collective even-even nuclei, it is argued that observables, such as yrast excitation energies and transition strengths, are nevertheless well described. From the present data, approximate lifetimes for the  $2_1^+$  and  $(4_1^+)$  states were extracted through a Doppler-shift analysis, and found to be consistent with the results of LNPS-new shell-model calculations.

The  $^{71}\text{Co}$  secondary beam was produced from projectile fragmentation of a 140 MeV/u stable  $^{82}\text{Se}$  beam provided by the Coupled Cyclotron Facility at NSCL [13], impinging on a 446 mg/cm $^2$   $^9\text{Be}$  production target and separated using a 240 mg/cm $^2$  Al degrader in the A1900 fragment separator [14]. The momentum acceptance of the separator was restricted to 2%, yielding on-target rates of typically 65  $^{71}\text{Co}$ /s. About 9.5% of the beam was  $^{71}\text{Co}$ , with  $^{72,73}\text{Ni}$  and  $^{74}\text{Cu}$  as the most intense components.

The secondary  $^9\text{Be}$  reaction target (376 mg/cm $^2$  thick) was located at the target position of the S800 spectrograph. Reaction products were identified on an event-by-event basis at the S800 focal plane with the standard detector systems [15]. The particle identification was performed with the measured energy loss and time-of-flight information, as demonstrated in [16], for the equivalent reaction on a  $^{61}\text{V}$  projectile beam. The inclusive cross section for the one-proton removal from  $^{71}\text{Co}$  to  $^{70}\text{Fe}$  was deduced to be  $\sigma_{inc} = 11.0(8)$  mb.

The high-resolution  $\gamma$ -ray detection system GREYINA [17, 18], an array of 36-fold segmented high-purity germanium detectors grouped into modules of four crystals each, was used to measure the prompt  $\gamma$  rays emitted by the reaction residues. The nine detector modules available at the time were arranged in two rings, with four located at  $58^\circ$  and five at  $90^\circ$  with respect to the beam axis. Online signal decomposition provided  $\gamma$ -ray interaction points for event-by-event Doppler reconstruction of the photons emitted in-flight [18] at  $v/c = 0.4$ . The information on the momentum vector of projectile-like reaction residues, as ray-traced through the spectrograph, was incorporated into the Doppler reconstruction. Fig. 1(a) provides the Doppler-reconstructed  $\gamma$ -ray spectrum for  $^{70}\text{Fe}$  produced with nearest-neighbor addback included [18]. The remarkable peak-to-background ratio enabled spectroscopy at modest levels of statistics in a nucleus far removed from stability. In addition to the previously reported  $2_1^+ \rightarrow 0_1^+$  and  $(4_1^+) \rightarrow 2_1^+$  transitions [8, 9], one additional  $\gamma$  ray, at 1110(4) keV, could be identified in  $^{70}\text{Fe}$ .

GREYINA's  $\gamma\gamma$  coincidence capability resulted in the level scheme displayed in the inset to Fig. 1(a). Figure 1(b) presents the spectrum in coincidence with the 857-keV transition, returning the other two  $\gamma$  rays. Together with the peak intensities, this places the three

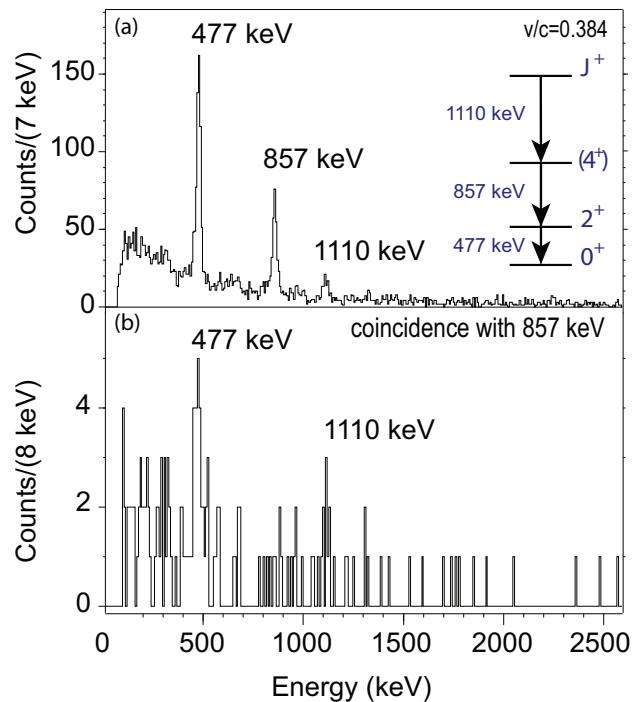


FIG. 1: (a) Doppler-reconstructed  $\gamma$ -ray spectrum in coincidence with  $^{70}\text{Fe}$  reaction residues. (b)  $\gamma\gamma$  coincidence spectrum gated on the 857-keV transition, returning peaks at 477 and 1110 keV, leading to the proposed level scheme in the inset of (a).

transitions in a cascade as indicated in Fig. 1(a).

The photopeak efficiency of GREYINA was calibrated with standard sources and corrected for the Lorentz boost of the  $\gamma$ -ray distribution emitted by the residual nuclei moving at almost 40% of the speed of light. The fact that one crystal in a forward detector module was not working was taken into account. The peak areas were determined from the spectrum of  $^{70}\text{Fe}$  without addback, avoiding uncertainties associated with the addback efficiency [18]. Partial proton-removal cross sections to the specific final states were determined from the efficiency-corrected  $\gamma$ -ray peak areas, with discrete feeding subtracted, relative to the number of incoming  $^{71}\text{Co}$  projectiles and the number density of the target:  $\sigma(0^+) = 1.0(6)$  mb,  $\sigma(2^+) = 4.0(8)$  mb,  $\sigma(4^+) = 4.1(6)$  mb, and  $\sigma(J^+) = 1.85(30)$  mb.

One-nucleon removal is a direct reaction with sensitivity to single-particle degrees of freedom. The cross sections for the population of individual  $^{70}\text{Fe}$  final states depend sensitively on the projectile to final-state one-body overlaps and on their normalizations; i.e., the spectroscopic factors [10]. Shell-model calculations with the LNPS-new effective interaction predict a  $7/2^-$   $^{71}\text{Co}$  ground state, in agreement with  $\beta$ -decay results [19], and a low-lying (200 keV)  $1/2^-$  isomer that has not yet been observed.

Using the one-nucleon removal methodology detailed

in Ref. [20] together with the LNPS-new [1, 11] spectroscopic factors for incident  $^{71}\text{Co}$  in the  $7/2^-$  and  $1/2^-$  states, the partial cross sections to bound  $^{70}\text{Fe}$  shell-model final states were calculated and confronted with experiment in Fig. 2. With reference to the nucleon removal reaction systematics [21], a reduction factor  $R_s = 0.4(1)$  was assumed between the calculated and the measured cross sections, based on the final-states yields-weighted proton separation energy,  $S_p \approx 18$  MeV, resulting in a proton and neutron separation energy asymmetry of  $\Delta S = S_p - S_n \approx 12$  MeV for  $^{71}\text{Co}$  [22]. The presence of both the ground and the isomeric state in the incoming  $^{71}\text{Co}$  beam cannot be ruled out and the measured cross section distribution may correspond to a linear combination of both.

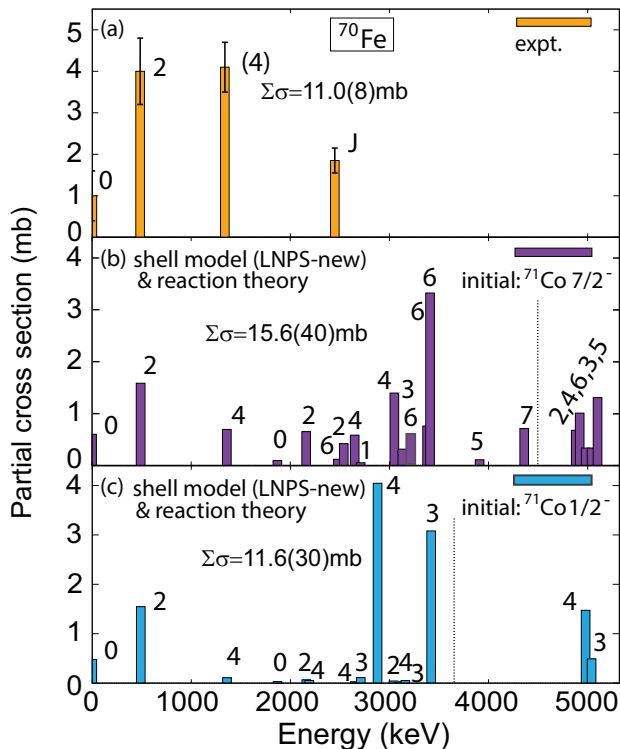


FIG. 2: Partial proton removal cross sections from  $^{71}\text{Co}$  for the population of positive-parity  $^{70}\text{Fe}$  final states: experiment (a) and calculations assuming the  $7/2^-$  (b) and  $1/2^-$  (c) shell-model initial states of the  $^{71}\text{Co}$  projectile and  $R_s$ . The calculated cross sections indicated beyond the dashed lines correspond to the summed strengths to bound states for the given  $J^+$  values at high excitation energy, placed here at 5 MeV.

For both possible initial states, the predicted population pattern is at odds with that measured and with the simple  $\gamma$ -ray spectrum observed. A strong population of high-lying states, such as the  $6_4^+$ ,  $4_4^+$  or  $3_3^+$  levels, would lead to the presence of several strong additional transitions, connecting the populated high-lying states to the level scheme reported here. For each assumed  $^{71}\text{Co}$  initial state, the sums of the partial cross sections to all bound

shell-model final states below  $S_n = 5.32(64)$  MeV [22] are  $\sigma_{inc}^{7/2^-} = 15.6(40)$  mb and  $\sigma_{inc}^{1/2^-} = 11.6(30)$  mb, slightly higher than the measured inclusive cross section of  $\sigma_{inc} = 11.0(8)$  mb.

The apparent simplicity of the observed population of final states in  $^{70}\text{Fe}$  is rather puzzling. We note that the  $\gamma$ -ray spectrum reported here is consistent with that reported from the  $(p, 2p)$  reaction, where no  $\gamma$  rays other than those associated with the  $2_1^+ \rightarrow 0_1^+$  and  $(4_1^+) \rightarrow 2_1^+$  transitions were observed [9]. While the cross sections from our  $^9\text{Be}$ -induced proton removal and  $(p, 2p)$  may differ quantitatively, qualitatively they will populate the same proton-hole configurations and the respective cross sections should scale with the same spectroscopic factors. The modest energy resolution accomplished with a scintillator array in the  $(p, 2p)$  measurement of Ref. [9] likely prevented the identification of the (weak) 1110-keV peak due to a disadvantage in the peak-to-background ratio. However, their superior detection efficiency should have enabled the clear observation of intense feeding transitions from high-lying states in view of their predicted strong population. Such concentration of proton spectroscopic strength in low-lying yrast states in the  $N = 40$  region has also been reported for other proton removal reactions leading to  $^{66,68}\text{Fe}$  [23],  $^{60}\text{Ti}$  [16] and  $^{66}\text{Cr}$ ,  $^{72}\text{Fe}$  [9].

One must consider the pandemonium effect [12], a situation where modestly efficient  $\gamma$ -ray spectroscopy of discrete transitions misses the population of high-lying states ultimately de-exciting to the yrast states through a large number of weak transitions. This effect, thus, attributes high-lying strengths to the yrast states that act as collectors for weak feeding transitions escaping observation. This is a possibility given the extreme level density predicted by the shell-model - with more than 100 states below  $S_n = 5.32$  MeV in  $^{70}\text{Fe}$  - but would actually require a larger fragmentation of the strength than that predicted. Specifically, further fragmentation would be expected beyond that to one or two high-lying states as the latter would certainly have their strongest transitions observed. Such a scenario of sizable fragmentation could also explain the slight mismatch between the calculated and measured inclusive cross sections, as increased fragmentation would likely shift spectroscopic strength to energies beyond  $S_n$ . Hence, an understanding of spectroscopic strengths in even-even nuclei of the  $N = 40$  island of inversion may demand yet larger model spaces and more complex, mixed configurations, requiring the inclusion of orbitals beyond  $\nu g_{9/2}$  and  $\nu d_{5/2}$  that were already identified as critical for describing the region [1]. Assuming such an interpretation of the present data, we suggest the newly established level at 2448(4) keV to correspond to the  $(6_1^+)$  state or a higher-lying  $4^+$  state. The energies of the transitions from the  $2^+$  and  $4^+$  states reported in the  $\beta$ -decay work [8] were used here to deduce the level energy due to a significant sensitivity to excited-state lifetimes in the present in-beam data, as

discussed below. For the two possible  $^{71}\text{Co}$  initial states, the strongly populated  $6^+$  levels ( $7/2^-$  initial state) and  $4^+$  and  $3^+$  levels ( $1/2^-$  isomeric initial state) would, in a pandemonium picture, ultimately feed into the yrast  $6_1^+$  and  $4^+$  states. We note the very good agreement with the LNPS-new shell-model calculation that places the  $6_1^+$  state at 2.48 MeV, within 30 keV of the measured value proposed here, while the closest higher-excited  $4^+$  is predicted to be located 200 keV higher.

Unlike any other shell-model effective interaction for this mass region, LNPS(-new) [1, 11] has demonstrated predictive power for collective observables, such as for the  $B(E2)$  transition strengths and energies of the lowest-lying  $2^+$  and  $4^+$  states [1, 9, 16, 24, 25]. For the measurements reported here, the  $\gamma$ -ray spectra reveal effects attributed to excited-state lifetimes that can inform on the expected collectivity of  $^{70}\text{Fe}$ . The inset of Fig. 3(a) demonstrates a distinct shift in energy of the  $2_1^+ \rightarrow 0_1^+$  transition detected in the GRETTINA detectors mounted in the  $58^\circ$  and  $90^\circ$  rings when corrected for the Doppler shift assuming the mid-target beam velocity. This indicates that the  $2_1^+$  state decays on average with a velocity lower than the mid-target one; i.e., when the  $^{70}\text{Fe}$  ions lost more energy. This is also the reason for the mismatch between the transition  $\gamma$ -ray energy reported here and that from  $\beta$  decay, 477 keV vs. 483 keV. Using GEANT [26], the lifetimes can be determined by matching to simulations the peak shapes and peak positions observed in detector groups at different polar angles, such as forward and  $90^\circ$ . We note that for long lifetimes the peak shape and peak position are impacted while shorter lifetimes largely affect the peak position only. Essential for this simulation is the precise knowledge of the transition energy and the target position along the beam axis. A target offset of 0.3(3) mm downstream from the center of GRETTINA was determined with the help of a known  $\gamma$ -ray transition in a contaminant. This value is small as compared to the actual  $\approx 2$  mm target thickness. Using the transition energies of 483 and 855 keV from  $\beta$  decay [8] and the target offset, effective lifetimes for the  $2_1^+$  and  $4_1^+$  states were extracted from a log likelihood minimization procedure that takes into account the feeding by the  $4^+$  level (the 1110 keV transition was too weak for such an analysis and was assumed to be prompt). The results are shown in Fig. 3, where the spectra for each ring of GRETTINA are overlaid with the GEANT simulation that minimized the negative log-likelihood surface, given as an inset (Fig. 3(b)). To illustrate the sensitivity of the present measurement to the different lifetimes in more detail, Fig. 4 provides simulated line shapes for the two transitions of interest for various lifetime values. For longer lifetimes, the primary sensitivity is to the tails of the peak shape, while shorter lifetimes affect the positions of the peak maximum. We note that similar sensitivity studies for other beam and target combinations

simulated for the AGATA array can be found in [27].

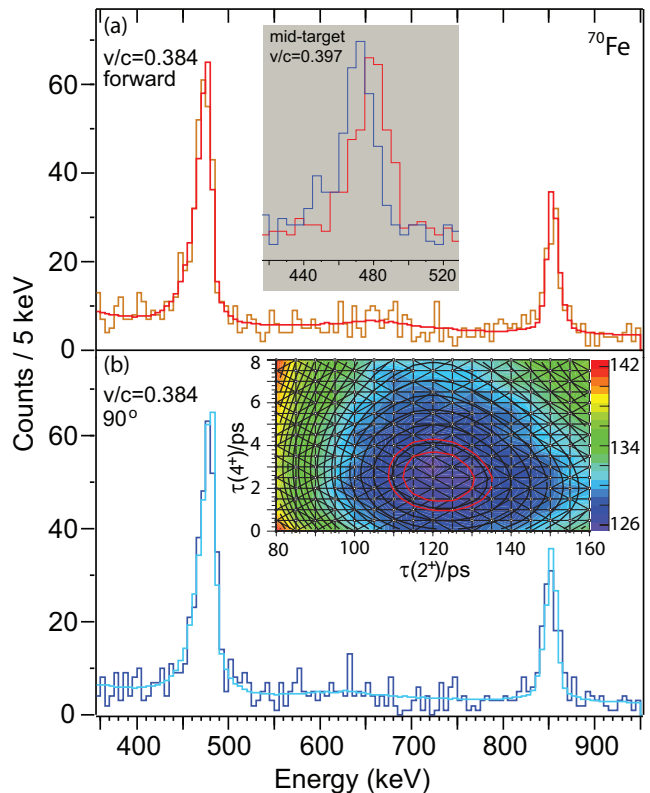


FIG. 3: Doppler-corrected  $\gamma$ -ray spectra from GRETTINA's forward ( $58^\circ$ ) and  $90^\circ$  rings ( $v/c = 0.384$ ; the  $4_1^+ \rightarrow 2_1^+$  transition lines up in both rings). A significant energy difference is observed for the  $2_1^+ \rightarrow 0_1^+$  transition at the mid-target  $v/c$  (top inset). Overlaid are GEANT simulations that minimize a negative log-likelihood surface (bottom inset) of a fit to a large set of simulated lifetimes properly accounting for the  $4_1^+$  feeding of the  $2_1^+$  state.

The deduced effective lifetimes (95% confidence interval for the fit) are  $\tau_{\text{eff}}(2_1^+) = 120_{-11}^{+15}$  ps and  $\tau_{\text{eff}}(4_1^+) = 2.3 \pm 1.5$  ps, respectively. Adding the systematic uncertainty from the target offset increases the error range of the longer lifetime to  $\tau_{\text{eff}}(2_1^+) = 120 \pm 20$  ps. These lifetimes have to be considered as effective ones since the yrast cascade is, most likely, subject to significant unobserved feeding from higher-lying states which could lead to an overestimation of the lifetimes. Given these uncertainties, one may conservatively conclude that the observed lifetime effects are consistent with a  $\tau(2_1^+)$  value of order 100 ps and  $\tau(4_1^+) \approx 2 - 4$  ps. This is in broad agreement with the LNPS shell-model calculations of the corresponding  $B(E2)$  values quoted in Ref. [9] from which  $\tau(2_1^+) = 81$  ps and  $\tau(4_1^+) = 3$  ps are extracted when using the measured transition energies. This underlines the collective nature of  $^{70}\text{Fe}$  as well as the success of the LNPS shell-model calculations [1, 11] in the description of this hallmark property of a nucleus within the island of inversion.

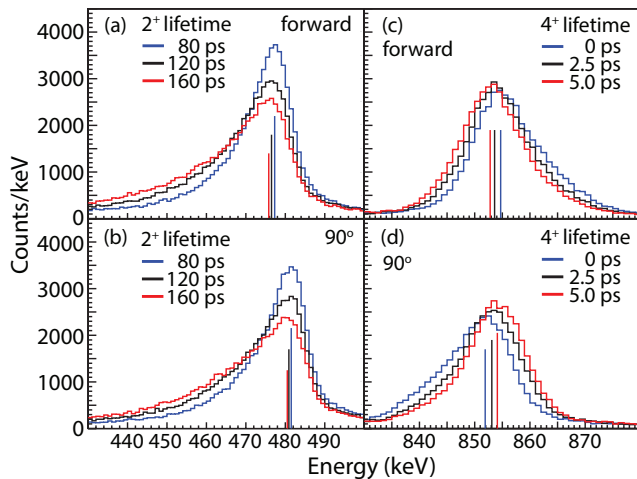


FIG. 4: Line shapes simulated with GEANT for different lifetimes of the  $2_1^+ \rightarrow 0_1^+$  transition in the (a) forward and (b)  $90^\circ$  detectors and for various lifetimes of the  $(4_1^+) \rightarrow 2_1^+$  transition in the (c) forward and (d)  $90^\circ$  detectors ( $v/c = 0.384$ ). This illustrates the specific sensitivities that the present measurement exhibits for the long  $\tau(2^+)$  (strong tails) and short  $\tau(4^+)$  (shifting peak position - indicated by vertical lines) values.

In summary, high-resolution in-beam  $\gamma$ -ray spectroscopy with GRETINA was performed for the neutron-rich nucleus  $^{70}\text{Fe}$  following one-proton removal from  $^{71}\text{Co}$  projectiles. A newly observed 1101(4)-keV  $\gamma$  ray was tentatively assigned to the transition from the  $(6_1^+)$  or a higher-lying  $(4^+)$  state at 2.448(4) MeV to the  $(4_1^+)$  level, based on comparison with the results of calculations using eikonal reaction theory incorporating spectroscopic factors from shell-model calculations based on the LNPS-new effective interaction. The  $(J^+) \rightarrow (4_1^+) \rightarrow 2_1^+$  cascade is found to agree well with the shell-model description if the newly discovered level is the  $6_1^+$  state. The pandemonium effect and an implied large fragmentation of spectroscopic strength are proposed to account for the marked discrepancy between measured and calculated population patterns: these present a challenge from an experimental and theoretical point of view. Despite these limitations, it was shown that besides the excitation energies, the shell-model calculations also account for another collective observable, the approximate excited-state lifetimes of the  $2_1^+$  and  $(4_1^+)$  states, extracted here via Doppler shifts and line shapes.

This work was supported by the US National Science Foundation (NSF) under Cooperative Agreement No. PHY-1565546 (NSCL) and grant No. PHY-1617250 (Ursinus), by the US Department of Energy (DOE) National Nuclear Security Administration under award numbers de-na0003180 and de-na0000979, and by the DOE-SC Office of Nuclear Physics under Grants DE-FG02-08ER41556 (NSCL), DE-FG02-97ER41041 (UNC), DE-FG02-97ER41033 (TUNL), and DE-AC02-06CH11357 (ANL). GRETINA was funded

by the DOE, Office of Science. Operation of the array at NSCL was supported by the DOE under Grant No. de-sc0014537 (NSCL) and DE-AC02-05CH11231 (LBNL). J.A.T. and S.J.F & D.K.S acknowledge the support of the Science and Technology Facilities Council (UK) grant ST/L005743/1 and ST/L005794/1, respectively. We also thank T.J. Carroll for the use of the Ursinus College Parallel Computing Cluster, supported by NSF grant No. PHY-1607335. A.P. is supported in part by MINECO (Spain) Grant FPA2014-57196 and the Severo Ochoa Programme SEV-2016-0597.

- 
- \* J. Belarge is currently an MIT Lincoln Laboratory employee. No Laboratory funding or resources were used to produce the result/findings reported in this publication.
- † Present address: Department of Physics, University of Massachusetts Lowell, Lowell, Massachusetts 01854, USA
- ‡ Present address: Dipartimento di Fisica, Università degli Studi di Milano, 20122 Milano, Italy
- [1] S. M. Lenzi, F. Nowacki, A. Poves, and K. Sieja Phys. Rev. C 82, 054301 (2010).
  - [2] F. Nowacki, A. Poves, E. Caurier, B. Bounthong, Phys. Rev. Lett. 117, 272501 (2016).
  - [3] A. Gade and S. N. Liddick, J. Phys. G 43, 024001 (2016).
  - [4] B. Alex Brown, Physics 3, 104 (2010).
  - [5] T. Sumikama, S. Nishimura, H. Baba, F. Browne, P. Doornenbal, N. Fukuda, S. Franchoo, G. Gey, N. Inabe, T. Isobe, P.R. John, H.S. Jung, D. Kameda, T. Kubo, Z. Li, G. Lorusso, I. Matea, K. Matsui, P. Morfouace, D. Mengoni, D.R. Napoli, M. Niikura, H. Nishibata, A. Odahara, E. Sahin, H. Sakurai, P.-A. Soderstrom, G.I. Stefan, D. Suzuki, H. Suzuki, H. Takeda, R. Taniuchi, J. Taprogge, Zs. Vajta, H. Watanabe, V. Werner, J. Wu, Z.Y. Xu, A. Yagi, K. Yoshinaga, Phys. Rev. C 95, 051601 (2017)
  - [6] A. Aprahamian, I. Bentley, M. Mumpower, and R. Surman, AIP ADVANCES 4, 041101 (2014).
  - [7] S. Brett, I. Bentley, N. Paul, R. Surman, and A. Aprahamian, Eur. Phys. J. A 48, 184 (2012).
  - [8] G. Benzoni, A.I. Morales, H. Watanabe, S. Nishimura, L. Coraggio, N. Itaco, A. Gargano, F. Browne, R. Daido, P. Doornenbal, Y. Fang, G. Lorusso, Z. Patel, S. Rice, L. Sinclair, P.-A. Soderstrom, T. Sumikama, J. Wu, Z.Y. Xu, R. Yokoyama, H. Baba, R. Avigo, F.L. Bello Garrote, N. Blasi, A. Bracco, F. Camera, S. Ceruti, F.C.L. Crespi, G. de Angelis, M.-C. Delattre, Zs. Dombradi, A. Gottardo, T. Isobe, I. Kuti, K. Matsui, B. Melon, D. Mengoni, T. Miyazaki, V. Modamio-Hoybjor, Phys. Lett. B 751, 107 (2015).
  - [9] C. Santamaria, C. Louchart, A. Obertelli, V. Werner, P. Doornenbal, F. Nowacki, G. Authalet, H. Baba, D. Calvet, F. Chateau, A. Corsi, A. Delbart, J.-M. Gheller, A. Gillibert, T. Isobe, V. Lapoux, M. Matsushita, S. Momiyama, T. Motobayashi, M. Niikura, H. Otsu, C. Peron, A. Peyaud, E. C. Pollacco, J.-Y. Rousse, H. Sakurai, M. Sasano, Y. Shiga, S. Takeuchi, R. Taniuchi, T. Uesaka, H. Wang, K. Yoneda, F. Browne, L. X. Chung, Zs. Dombradi, S. Franchoo, F. Giacoppo, A. Gottardo, K. Hadynska-Klek, Z. Korkulu, S. Koyama, Y. Kubota,

- J. Lee, M. Lettmann, R. Lozeva, K. Matsui, T. Miyazaki, S. Nishimura, L. Olivier, S. Ota, Z. Patel, N. Pietralla, E. Sahin, C. Shand, P.-A. Söderström, I. Stefan, D. Steppenbeck, T. Sumikama, D. Suzuki, Zs. Vajta, J. Wu, and Z. Xu, *Phys. Rev. Lett.* 115, 192501 (2017).
- [10] J. A. Tostevin, *J. Phys. G: Nucl. Part. Phys.* 25, 735 (1999) and P. G. Hansen and J. A. Tostevin, *Annu. Rev. Nucl. Part. Sci.* 53, 221 (2003).
- [11] F. Nowacki (private communication).
- [12] J. C. Hardy, L. C. Carraz, B. Jonson, P. G. Hansen, *Phys. Lett. B* 71, 307 (1977).
- [13] A. Gade and B. M. Sherrill, *Phys. Scr.* 91, 053003 (2016).
- [14] D. J. Morrissey *et al.*, *Nucl. Instrum. Methods in Phys. Res. B* 204, 90 (2003).
- [15] D. Bazin *et al.*, *Nucl. Instrum. Methods in Phys. Res. B* 204, 629 (2003).
- [16] A. Gade, R.V.F. Janssens, D. Weisshaar, B.A. Brown, E. Lunderberg, M. Albers, V.M. Bader, T. Baugher, D. Bazin, J.S. Berryman, C.M. Campbell, M.P. Carpenter, C.J. Chiara, H.L. Crawford, M. Cromaz, U. Garg, C.R. Hoffman, F.G. Kondev, C. Langer, T. Lauritsen, I.Y. Lee, S.M. Lenzi, J.T. Matta, F. Nowacki, F. Recchia, K. Sieja, S.R. Stroberg, J.A. Tostevin, S.J. Williams, K. Wimmer, and S. Zhu, *Phys. Rev. Lett.* 112, 112503 (2014).
- [17] S. Paschalis *et al.*, *Nucl. Instrum. Methods Phys. Res. A* 709, 44 (2013).
- [18] D. Weisshaar, D. Bazin, P. C. Bender, C. M. Campbell, F. Recchia, V. Bader, T. Baugher, J. Belarge, M. P. Carpenter, H. L. Crawford, M. Cromaz, B. Elman, P. Fallon, A. Forney, A. Gade, J. Harker, N. Kobayashi, C. Langer, T. Lauritsen, I. Y. Lee, A. Lemasson, B. Longfellow, E. Lunderberg, A. O. Macchiavelli, K. Miki, S. Momiyama, S. Noji, D. C. Radford, M. Scott, J. Sethi, S. R. Stroberg, C. Sullivan, R. Titus, A. Wiens, S. Williams, K. Wimmer, and S. Zhu, *Nuclear Instrum. Methods Phys. Res. A* 847, 187 (2017).
- [19] M. M. Rajabali, R. Grzywacz, S. N. Liddick, C. Mazzocchi, J. C. Batchelder, T. Baumann, C. R. Bingham, I. G. Darby, T. N. Ginter, S. V. Ilyushkin, M. Karny, W. Krolas, P. F. Mantica, K. Miernik, M. Pfützner, K. P. Rykaczewski, D. Weisshaar, and J. A. Winger, *Phys. Rev. C* 85, 034326 (2012)
- [20] A. Gade, P. Adrich, D. Bazin, M. D. Bowen, B. A. Brown, C. M. Campbell, J. M. Cook, T. Glasmacher, P. G. Hansen, K. Hosier, S. McDaniel, D. McGlinchery, A. Obertelli, K. Siwek, L. A. Riley, J. A. Tostevin, and D. Weisshaar, *Phys. Rev. C* 77, 044306 (2008).
- [21] J. A. Tostevin and A. Gade, *Phys. Rev. C* 90, 057602 (2014).
- [22] M. Wang, G. Audi, A.H. Wapstra, F.G. Kondev, M. MacCormick, X. Xu, B. Pfeiffer, *Chin. Phys. C* 36, 1603 (2012).
- [23] P. Adrich, A. M. Amthor, D. Bazin, M. D. Bowen, B. A. Brown, C. M. Campbell, J. M. Cook, A. Gade, D. Galaviz, T. Glasmacher, S. McDaniel, D. Miller, A. Obertelli, Y. Shimbara, K. P. Siwek, J. A. Tostevin, and D. Weisshaar, *Phys. Rev. C* 77, 054306 (2008).
- [24] A. Gade, R. V. F. Janssens, T. Baugher, D. Bazin, B. A. Brown, M. P. Carpenter, C. J. Chiara, A. N. Deacon, S. J. Freeman, G. F. Grinyer, C. R. Hoffman, B. P. Kay, F. G. Kondev, T. Lauritsen, S. McDaniel, K. Meierbachtol, A. Ratkiewicz, S. R. Stroberg, K. A. Walsh, D. Weisshaar, R. Winkler, and S. Zhu, *Phys. Rev. C* 81, 051304(R) (2010).
- [25] W. Rother, A. Dewald, H. Iwasaki, S. M. Lenzi, K. Starosta, D. Bazin, T. Baugher, B. A. Brown, H. L. Crawford, C. Fransen, A. Gade, T. N. Ginter, T. Glasmacher, G. F. Grinyer, M. Hackstein, G. Ilie, J. Jolie, S. McDaniel, D. Miller, P. Petkov, Th. Pissulla, A. Ratkiewicz, C. A. Ur, P. Voss, K. A. Walsh, D. Weisshaar, and K.-O. Zell, *Phys. Rev. Lett.* 106, 022502 (2011).
- [26] UCGretina GEANT4, L. A. Riley, Ursinus College, unpublished.
- [27] C. Domingo-Pardo, D. Bazzacco, P. Doornenbal, E. Farnea, A. Gadea, J. Gerl, H. J. Wollersheim, *Nucl. Instrum. Methods Phys. Res. A* 694, 297 (2012).